Discretization of Continuous Spaces using Barycentric Subdivision Method with Metric Space Constraints on the Nearest Neighbour Edges

E. E. Audu[1*], A. A. Eteng[2], I. Uchendu[2,3]

[1]Department of Innovation Development, Research, Technology and Technology (RTI), Abuja, Nigeria.
[2]Department of Electrical/Electronic Engineering, University of Port Harcourt, Rivers State, Nigeria.
[3]Electromagnetic Fields Group, University of Colorado, Boulder, USA.

ABSTRACT: The Rao-Wilton-Glisson (RWG) is a commonly used basis function in the numerical solution of the electric field integral equation (EFIE) using the Method of Moments (MoM) and Galerkin approach. This method relies on triangular patches to approximate the surface current. Traditionally, barycentric subdivision of a primary triangle into ***n***-sub-triangles has been used with RWG basis function to solve the EFIE using MoM. This paper presents a method of approximating a surface using triangular patches by sub-dividing a primary triangle into (***2n-1***) sub-triangles. which creates a denser mesh than the widely used nine (9) points quadrature method. The structure is approximated by small square patches, which are further sub-divided into two primary triangles. By applying barycentric sub-division, the primary triangles are decomposed into sub-triangles to create a mesh over the surface of the structure. Using graph theory, the triangular meshes are defined by the function, **G (V, E)**, where V and E are the vertices and edges of the triangles in the mesh space, respectively. The connectivity matrix of shared edges is found by imposing a constraint on the edge length using metric spaces. This method approximates a square patch with 32 scalene triangles and shows that it can be used to reconstruct equilateral patches and doubly split double ring into mesh structures.

KEYWORDS: Electric field integral equation; Barycentric subdivision, Method of Moments; Rao-Wilton-Glisson basis function; Discretization of spaces; Solid and Object representations; computational geometry.

[Received July. 15, 2024; Revised Sep. 3, 2024; Accepted Sep. 9, 2024] Print ISSN: 0189-9546 | Online ISSN: 2437-2110

I. INTRODUCTION

In many applications involving integral or differential equations that prove to be analytically intractable or difficult to solve, it is often convenient to solve the problem using numerical approaches. In electromagnetic scattering problems, numerical solutions are often employed to characterize the scattering properties of conducting and non-conducting objects of arbitrary shapes (Li et al., 2021; Li and Li, 2004; Wilton et al., 1982; Rao et al., 1982). Among many numerical approaches such as the Finite Element Method and Finite Difference Time Domain, the Method of Moments (MoM) is arguably the most commonly and widely used numerical method due to its ability to yield accurate results at arbitrary frequencies (Rao, 2024; Li et al., 2021.

The electric field integral equation (EFIE) is a mathematical formulation that describes the scattering problem for an arbitrary shaped object in the pool of electromagnetic fields. The MoM, with Rao-Wilton-Glisson (RWG) basis functions via the Galerkin approach, has been applied to solve EFIE (Zhu et al., 2014; Chung et al., 2004). This method involves discretization and meshing of the objects of any shape in three-dimensions (3D) and two-dimensions (2D) into patches for basis function operations (Gurel et al, 2009). The MoM is used to solve time domain scattering problems formulated in terms of integral equations by expanding the equation into a series of basis function and unknown coefficients (Rao, 2024; Øyre, 2021). In this method, an equation formulated in either differential or integral form can be approximated by a matrix equation in a finite dimensional sub-space (Harrington, 1987).

The RWG basis function is well suited for use in the MoM expanded basis function expression to develop computational codes to describe the surface current on an object (Wilton et al., 1982; Rao et al., 1982). In the RWG basis function approach, the object is discretised into triangular surface patches to approximate the surfaces, which, in turn, represent the surface currents. Various studies have been extensively conducted on EFIE equations using RWG-based MoM and Galerkin method. RWG solvers for time harmonic and transient sources have been studied in great details (Lu et al, 2002). Also, the use of non-conforming scheme of RWG discretization with EFIE for closed conductor with no constraint imposed on the edge continuity has demonstrated (Ubeda et al, 2014; Ubeda et al, 2014). Different basis function scheme has been developed that are compatible with RWG basis function such has the multiresolution basis function consisting of linear combination RWG (Andriulli et al., 2008). This multiresolution scheme is well conditioned to address low frequency problems and can be applied to any mesh utilizing triangular facets for three-

Corresponding author: ideologye@yahoo.com
doi: http://dx.doi.org/10.4314/njtd.v21i3.2742

dimensional objects. Bertrand et al. (2019) developed RWG basis function with MoM to study and improve the performance and flexibility of a substrate integrated waveguide. As highlighted, the development of the RWG-based MoM relies on the generation of meshes that approximate the surfaces of the object. The RWG is then defined on the mesh which is a low-order basis function, which ensures continuity of normal currents only to common edges in the structure (Ubeda et al., 2020; Wilton et al., 1982). Consequently, a mesh generation algorithm which requires the use of mathematical functions, interpolations, and coordinate dissection is a significant component EFIE with the RWG-based MoM solutions.

Various methods of discretizing objects have been developed to make it possible to represent surfaces as a graph of triangular or polygon faces by connecting points on the surfaces where local information is embedded in the vertices of the structure (Liu et al., 2023). Such a simplistic way of representation enabled better way of modelling objects in two- and three-dimensions. Point clouds and meshes are two of the commonly conventional methods used in representation due to their efficiency (Peng et al., 2021). Unlike meshes where points are connected and information is encoded in the vertices, point clouds are lightweight and do not encode the information about the surface directly (Peng et al., 2021). However, the mesh method of object reconstruction provides clearer appearance and generate more information which can be used to supplement cloud-based approach (Wongwaen et al., 2012).

This paper focuses on the mesh method of surface representation in two-dimensional structures where points (also called vertices) are connected via edges. Vertice information can be used to sub-divide edges in the barycentric method of sub-dividing triangles. Various methods and techniques have been developed to geometrically represent surfaces or the location of vertices, such as generalised mean value coordinate for constructing interpolant in closed polygons and closed triangular meshes (Ju et al., 2023); and the mean value coordinates for triangular meshes (Thiery et al., 2012). Interpolation is an important concept in both finite elements and MoM for accurate evaluation of Green's function, surface current and division of objects (Koam et al., 2020; Luo et al., 2020; Blue et al., 2004). This concept plays an important role in graphical operations when inserting a new vertex or sub-dividing an edge into many partitions (Koam et al, 2020). The triangular patch is an important object in the RWG-based MoM, where the basis function is defined. Studies show that methods such as barycentric sub-division can be used to generate sub-triangles from a given primary triangle. For instance, a barycentric subdivision of a tetrahedron structure revealed that a dense set of smaller tetrahedrons can be produced thereby (Luo et al., 2020). The barycentric subdivision method of nine-point quadrature is commonly in the RWG-based MoM numerical solutions of the EFIE (Xiang et al., 2020).

The goal and novelty of this paper is to demonstrate the sub-division of a triangle into sixteen (16) quadrature points and approximate a square patch with thirty-two (32) triangular patches (quadrature points). Also, we show that the sub-division of triangular patches can be used to approximate circular structures such as doubly split double ring resonators for the design of metasurfaces. The sub-division of a triangle into sixteen (16) sub-triangles is provides a denser approximation than a nine (9) quadrature point sub-subdivision. Section II describes the formulation and method for surface meshing. In section III, the result of the meshing program is presented and discussed. Section IV provides the summary and conclusion of the work.

II. METHODS

In this section, the theoretical and mathematical basis for meshing a given perfectly square patch into two primaries triangles and subdividing the each of the primary triangles into sub-triangles is presented.

A. Method of moments

The method of Moments (MoM) provides a numerical computational technique for integro-differential equations and has been successfully applied in computing electromagnetic problems associated with radiation and scattering problems (Taboada et al., 2004; Harrington and Harrington, 1996, Rao et al., 1982; Makarov, 2002, Glibson, 2007). The method has been used to efficiently solve scattering problems of surfaces with different geometrical configurations and shapes (Wilton et al., 1979). With a proper choice of weighting functions, MoM discretizes field integral equations into a set of linear equations, and computes surface currents with great accuracy, with no dependence on the physical dimension of the scatterer (Tanaka et al., 2021; Taboada et al., 2004). The method is based on weighted residuals, where the unknown function is expanded in terms of unknown coefficients (Makarov, 2002; Glibson, 2007. Let us consider an integro-differential operator, L, acting on a current density, J, which is a consequence of a source term, g (Makarov, 2002, Glibson, 2007; Wilton et al., 1979) in Equations 1 - 26 analyze as follow;

$$L(J) = g \tag{1}$$

The unknown function can be expanded as a series sum of β and I at different basis values,

$$J = \sum_{k=1}^{N} \beta_n I_n \tag{2}$$

where N is the number of basis functions, or the number non-boundary vertices.

$$L \sum_{k=1}^{N} \beta_n I_n \approx g \tag{3}$$

The residual term is given as,

$$R - L \sum_{k=1}^{N} \beta_n I_n \tag{4}$$

Then,

$$\sum_{k=1}^{N} \beta_n L(I_n) = g \tag{5}$$

Let the weighting function be given as w_m (Harrington, 1996), then the inner product is defined as,

$$\sum_{k=1}^{N} \beta_n \langle w_m, L(I_n) \rangle = \langle w_m, g_n \rangle \tag{6}$$

In most scattering problems, the Galerkin method is often employed, where the weighting or testing function is the same as the basis function (Gassner and Winter, 2021; Sekulic et al., 2017; Glission, 2007; Sarkar et al., 2010; Harrington and Harrington, 1996, Rao et al., 1982; Makarov, 2002).
Thus,

$$w_m = I_m \tag{7}$$

$$\sum_{k=1}^{N} \beta_k \ \langle I_m, L(I_k) \rangle = \langle w_m, g_k \rangle \tag{8}$$

Eq. can be written in matrix form as.

$$[\beta_k][F_{mk}] = [g_k] \tag{9}$$

B. Rao-Wilton-Glisson (RWG) Basis Function

The current impressed by incident electromagnetic fields over inclusions and metallic surfaces of a cell structure depends on the geometrical structure of the surface. MoM based on the RWG basis function has been successful in solving scattering problems in electromagnetics (Chai et al., 2001; Kornprobst et al, 2019). The development of the RWG basis function was first credited to Glisson (Glisson, 1978, Wilton et al., 1980; Rao et al., 1982). The triangular patch RWG is the lowest, zeroth-order, basis function that supports continuity of normal current components across shared vertices of two adjacent triangles in current vector field calculations (Chai et al., 2001). Kronprobst et al. (2019) the success of the basis function to its suitable divergence conforming properties in the solution of Maxwell Equations (Kornprobst et al., 2019). RWG basis function supports surface current representation in two dimensions (2D) and three dimensions (3D).

The RWG basis function is used to expand then electric field integral equation (EFIE) by representing the current density in terms of the basis function which is well suited for triangular patches. Thus, the basis function is sometime called edge element because it is defined on two triangles, T_n^+ and T_n^-, with a common vertex, as shown in Fig.1 (Glisson, 1978, Wilton et al., 1980; Rao et al., 1982; Cvetkovic and Poljak, 2019). The RWG Basis function, I_n, defined on vertex n, is given as:

$$I_n = \begin{cases} \frac{l_n}{2A_n^+}\rho_n^+ \ , r \in T_n^+ \\ \frac{l_n}{2A_n^-}\rho_n^-, r \in T_n^- \\ 0, \ \text{Otherwise} \end{cases} \tag{10}$$

$$\nabla . I_n = \begin{cases} \frac{l_n}{A_n^+} \ , r \in T_n^+ \\ -\frac{l_n}{A_n^-}, r \in T_n^- \\ 0, \quad \text{Otherwise} \end{cases} \tag{11}$$

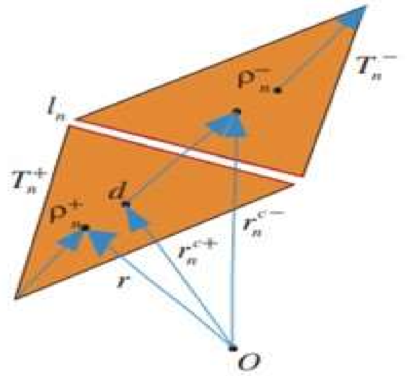

Fig.1. Triangular patch RWG showing Basis Function Parameters (Su et al., 2011)

where T_n^+ and T_n^- are the two triangles, ρ_n^+ and ρ_n^- are vectors defined between the free vertex and the barycenter of the triangles, r_n^{c+} *and* r_n^{c-} are centroid.

C. Graph theory and the notion of metric space.

A graph can be defined as a function consisting of a non-empty set of vertices, V, and set of edges that links all vertices, E. In general, a graph is compactedly denoted by G (V, E) where the vertex, V, is a set containing the list of all the vertices and the edge, E, is a set listing all the links between a pair of vertex in the structure. We consider a finite graph where elements belonging to the vertex and edge are finite. The elements in the vertex set are coordinates or location of points while the elements in the edge set are distance measurements between a pair of vertices.

Consider points on a surface which can be defined by a function, G (V, E), as a simple, non-directed and connected graph. Each vertex is defined by *d (x, y)*. Consequently, V can be defined as a set function.

$$V = \{(x_1, y_1), (x_2, y_2), (x_3, y_3), \dots\} \tag{12}$$

and the edge,

$$E = \{e_1, e_2, e_3, \dots\} \tag{13}$$

where (x_n, y_n) *and* e_n are elements of the set V and E respectively.

For a triangle with vertices, u, v, and w,

$$V = \{u, v, w\} \tag{14}$$

Then the edge,

$$E = \{e_{uv}, e_{uw}, e_{vw}\} \tag{15}$$

For $e_{uv} \in E$, the concept of metric space is introduced to determine the distance between any pair of edges from their coordinates. Consequently, the length, e_{uv}, between a vertex u and v can be defined in terms of a Euclidean distance,

$$e_{uv} = d(u, v) = \sqrt{(u_1 - v_1)^2 + (u_2 - v_2)^2} \tag{16}$$

Thus,

$$E = \{d(u,v), d(u,w), d(v,w), \ldots..\} \quad (17)$$

Let the primary triangles, $\triangle_+$ and $\triangle_-$, be sub-divided into 16 sub-triangles. Each of the 16 sub-triangles can be equally sub-divided into 16 equal sub-triangles. The density of triangles in H- space is proportional to the number of times a triangle is sub-divided. Thus, each of the triangles, $(\triangle_{\pm}^{j})_{j\in[1,16]}$, has a vertex and an edge associated with it. The triangular sub-division of $H \in \mathbb{R}^2$ can be formulated as a directed graph, G with a vertex, V, and an edge, E. Metric can be defined on the function, G (V, E). The function G (V, E) is a set in $H \in \mathbb{R}^2$. For each of the sub-triangles $\triangle_{\pm}^{j}$ there are three edges, $E = \{e_{uv}, e_{uw}, e_{vw}\}$. Therefore, the metric space is defined on the function, G, such that the points $u, v, w \in V$ in $\mathbb{R}^2$ space describes the position of each of the vertices in the discretized space. Let x, y define the coordinate of u in cartesian coordinate space. Then,

Definition 1.1. A metric space (V, E) consists of a non-empty set V and a function $d: G\text{x}G \to [0, \infty)$ such that the following conditions are satisfied.

I. $d(x,y) \geq 0$, $x, y \in G$. This implies that the length of the edges must be non-zero and positive number.

II. $d(x,y) = d(y,x)$. This defines the symmetry of distances and is true for all the length of edges as indicated in the Eqn. (3). For any two vertices located at (x_1, y_1) and (x_2, y_2), the Euclidean distance which the edge, $e_{1\to 2}$, is defined as,

$$d\left((x_1, x_2), (y_1, y_2)\right) = \sqrt{(x_2 - x_1)^2 + (y_2 - y_1)^2} \quad (18)$$

III. For the triangular inequality,

$$d\big((x_1, x_m), (y_1, y_m)\big) \leq \sqrt{(x_1 - x_m)^2 + (y_1 - y_m)^2} + \sqrt{(x_2 - x_m)^2 + (y_2 - y_m)^2} \quad (19)$$

Where x_m, y_m are the edges mid-point coordinates.

D. Barycentric subdivision

The notion of metric spaces on a set of coordinates was defined mathematically as a means to detect the nearest neighbour or vertex which is crucial in applying RWG basis function to differentiate between interior and non-interior vertices. Further to the concept of graph theory and metric spaces, the subdivision of all edges in a graph, G, which is the concept used to generate sub-triangles is discussed. Barycentric subdivision method takes a primary (major) triangle and subdivide into sub triangles. Each of new sub-triangle can be further subdivided into additional sub-triangles. Thus, in a barycentric sub-division method, a given triangle, T, is transformed into T_n where $n = \{1,2,3, \ldots k\}$ (Xiang et al., 2020; Diaconis and Miclo, 2010; Anisimov et al, 2016). Any of the ***n***-triangles can be randomly selected and barycentrically subdivided into six new sub-triangles. The process can be repeated many times provided that the chosen triangle is non-flat, and the sequence of this repeated sub-division gives rise to a Markov chain. In the RWG with MoM for EFIE, the primary triangle is sub-divided into nine (9) sub-triangles. To demonstrate how the use of barycentric method is applied in discretisation of surfaces, a perfectly square structure representing a section of an antenna structure is used. Let the function $H(l, w) \in \mathbb{R}^2$ define the square patch such that the following constraints $l = w$ and the Area, $A = l^2 = w^2$ are imposed on the H. Fig.2 shows the square patch to be discretized into two primary triangular patches.

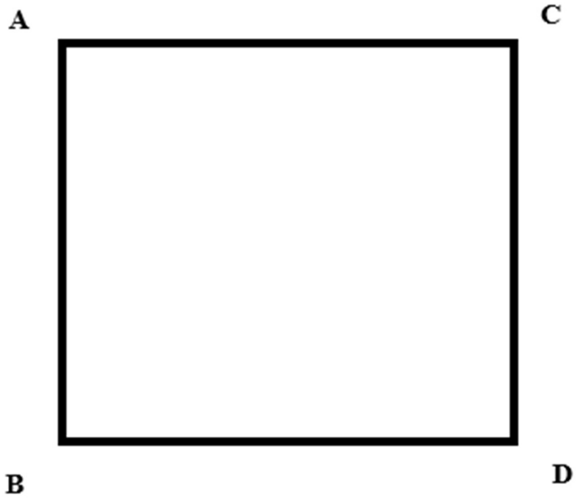

Fig.2. Square patch with vertices A, B, C and D.

Each of the vertices on the patch can be described as a point in x-y space on a rectangular coordinate system. Constructing line $|BC|$, partition the square patch into two primary triangles that are further barycentrically subdivided. Fig.3 and 4 show the two primary triangles and their corresponding edges emerged from partitioning the square patch.

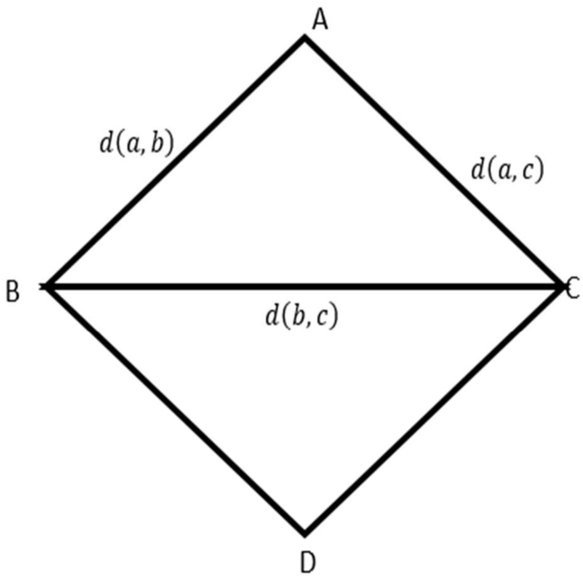

Fig.3. Square patch divided into primary triangles ABC and BCD

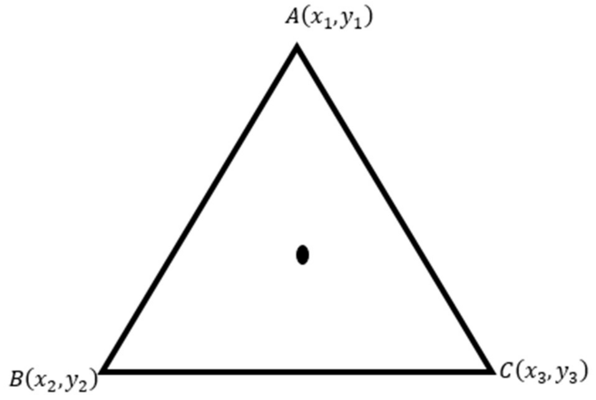

Fig. 4. Triangle with vertices A, B, and C.

The length of each of the edges $|AB|$, $|AC|$ and $|BC|$ can be computed using Eq. (18) as,

$$d\left((x_A, x_B), (y_A, y_B)\right) = |AB| = \sqrt{(y_2 - y_1)^2 + (x_2 - x_1)^2} \quad (20)$$

$$d\left((x_A, x_C), (y_A, y_C)\right) = |AC| = \sqrt{(y_3 - y_1)^2 + (x_3 - x_1)^2} \quad (21)$$

$$d\left((x_B, x_C), (y_B, y_C)\right) = |BC| = \sqrt{(y_3 - y_2)^2 + (x_3 - x_2)^2} \quad (22)$$

For equilateral triangles, the edge lengths are equal,

$$|AB| = |AC| = |BC| = \sqrt{(y_2 - y_1)^2 + (x_2 - x_1)^2} \quad (23)$$

In general, the mid-point of any vertex of a triangle can be calculated by averaging the length of an edge as,

$$m = \sqrt{\frac{\left(y_q - y_p\right)^2 + \left(x_q - x_p\right)^2}{4}} \quad (24)$$

Where $p = \{n, n+1\}$, $q = \{n+1, n+2\}$ and $n = \{1,2,3\}$ which is the vertices of a triangle.
The centroid of a triangle in fig.4 is given by,

$$x_c = \frac{1}{3}\sum_{n=1}^{3} x_n \quad (25)$$

$$y_c = \frac{1}{3}\sum_{n=1}^{3} y_n \quad (26)$$

Using Eq. (20) to Eq. (26), plane of projections can be constructed to create a new perspective about the triangle which form the basis of sub-division of edges as shown in fig.5. The points P_c and P_b are centroid and barycentre of the triangle respectively.

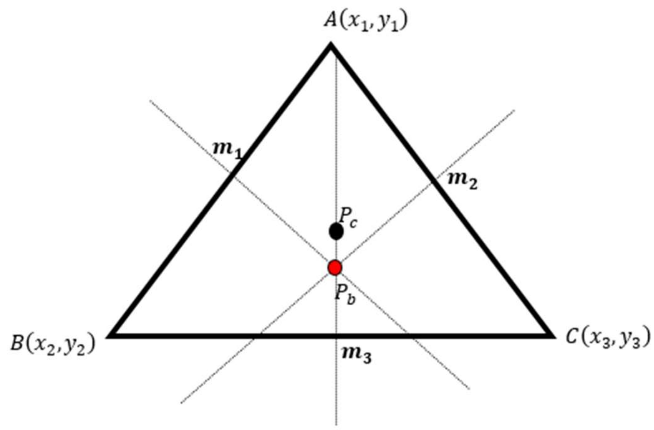

Fig.5. Projections of planes along the midpoint of the vertices.

By dividing edge $\overline{AB}$ in the middle, a new vertex m_1 is created along the point. Similarly, on edges $|AC|$ and $|BC|$, the new vertices are m_2 and m_3 respectively. We show that a given triangle can be sub-divided by considering mid-points of adjacent edges as shown in fig.6

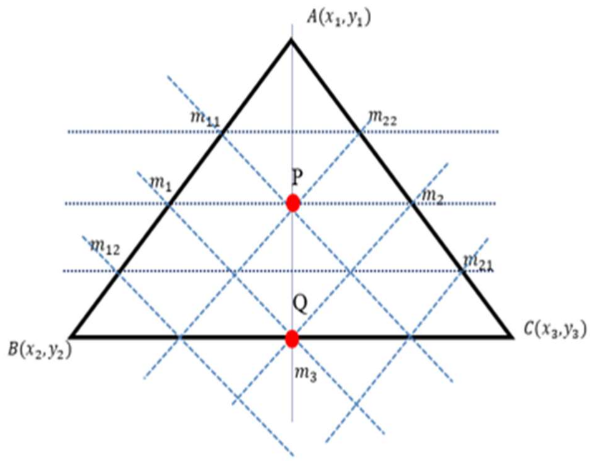

Fig.6. Bisecting of edge lengths of a triangle using midpoint.

To create sub-triangles from the primary triangle, the line $\overline{m_1 m_2}$ is first constructed from m_1 to m_2. The midpoints of $|Am_1|$, $|Bm_1|$, $|Am_2|$ and $|Cm_2|$ are m_{11}, m_{12}, m_{22} and m_{21} respectively partition $|AB|$ and $|AC|$ into four sections. This process of bisecting an edge can be repeated to the desire number of operations. As shown in fig.6, the main projections of lines from mid-point are made through point P and Q to construct 16 triangles. The lines intersect at different points forming sub-triangles.

The method of constructing edges and inserting vertices described above can be represented in terms of a flowchart in fig.7. Here, the step-by-step process of reconstructing the 2D mesh of a structure using triangular patches is presented.

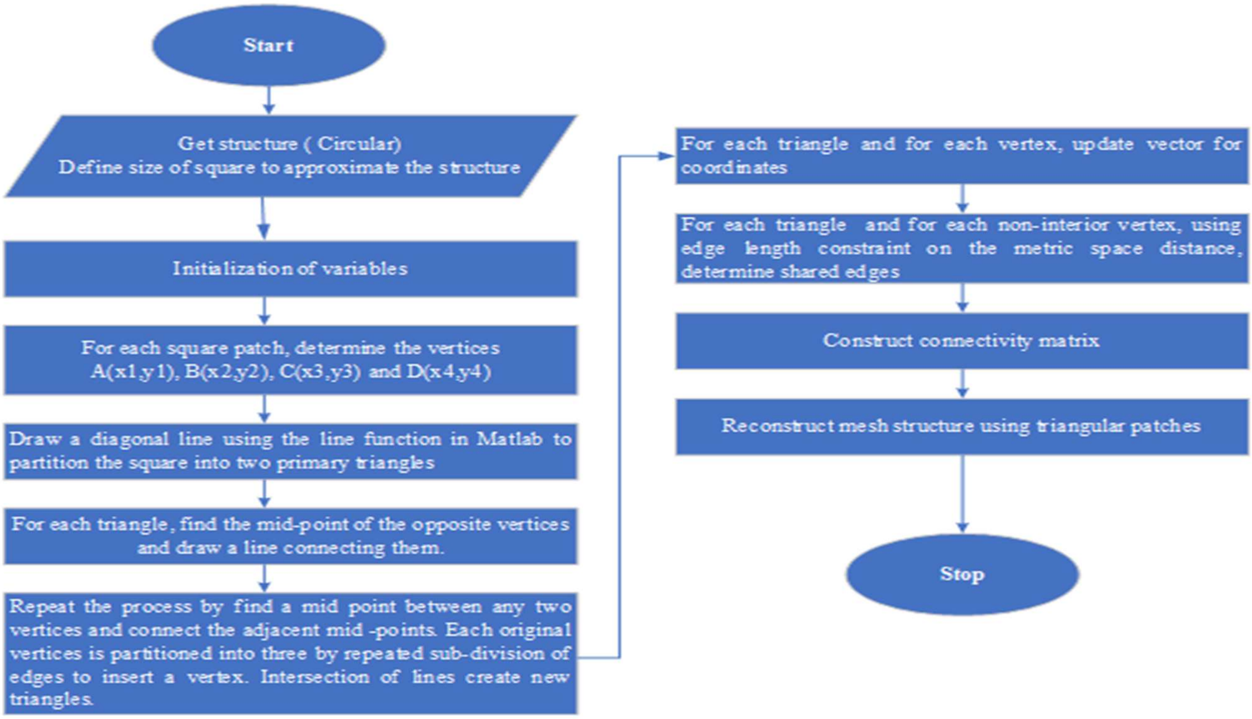

Fig. 7. Flowchart of mesh program for approximating circular or square patch structure using triangular patches

III. RESULTS AND DISCUSSION

The program to discretise a square patch surface into several connected triangular patches for numerically solving the electric field integral equation was developed using MATLAB. Specifically, concentric circular rings which share a structural similarity with a doubly split double ring resonator in metasurfaces.

A. Doubly Split double ring resonators.

This a unit cell structure consisting of two concentric split rings that can resonate at a certain frequency. The resonance frequency is a fundamental key performance parameter in the study of metasurfaces. Figs.8 and 9 are commonly used doubly split double ring resonators routinely used in the study of unit cell operations at different geometrical parameters and operating frequencies.

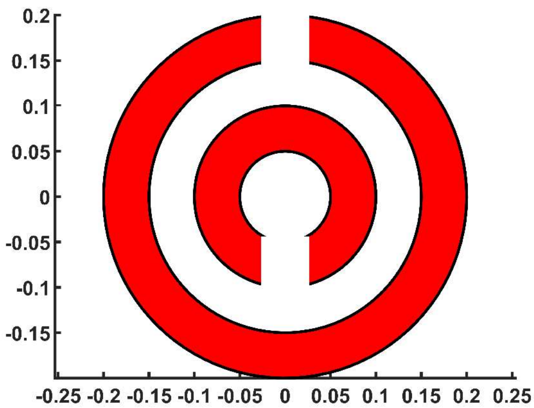

Fig. 8. circular doubly split double rings unit cell structure.

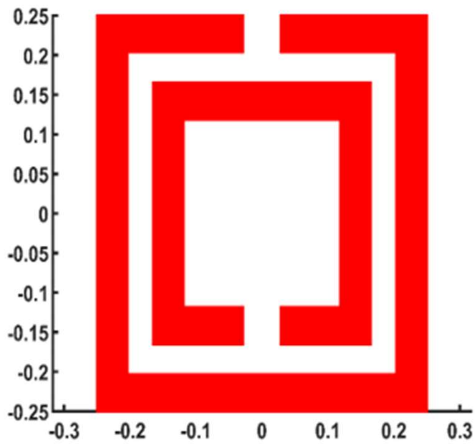

Fig.9. Square doubly split double rings unit cell structure.

To study the scattering of electromagnetic field and current distribution at resonant frequency, numerical solvers based on method of moments (MoM) relies on programs that can discretize the structure into triangular patches for the RWG basis function approach. Consequently, the structure to be discretised was cut into smaller square patches with well-defined coordinate location of each piece. Only the two-dimensional layout of the square patch structure was considered as the input parameter to the meshing program.

B. Mesh of square patch structure

Given the initial coordinates of the patch, (x_0, y_0), and the width of the structure, the dimension of the square patch is determined. The coordinates of the patch are (x_0, y_0), $(x_0 + h, y_0)$, $(x_0, y_0 + w)$ and $(x_0 + h, y_0 + w)$. The square patch was first partitioned into two primary isosceles triangles, called the upper and lower triangles. Each of the primary triangle was sub-divided into sixteen (16) sub-triangles by repeatedly partitioning the edges of the triangles as discussed previously. Using this method, a square patch is divided into a total of 32 scalene sub-triangles. Many square patches can be processed at the same time and re-assembled to provide a discrete approximation of the structure. Fig.10 shows a 10x10 mm square patch whose surface is sub-divided into 32 sub-triangles. The centroid of each of the sub triangles are marked which is an important aspect of RWG-basis function numerical calculations. Fig.11 shows the result of square patch structures at different dimensions. The first patch is 12 x 12 mm, the second patch has the dimension of 8 x 8 mm, and the third patch is 4 x 4 mm. The result indicates that when a triangle is sub-divided, and a sub-triangle is further sub-divided the sub-divided triangles tend to be smaller and flat. Eq. (27) shows a connectivity matrix of Fig.10 (b) which indicates common edges between a pair of triangles or indicate if vertices are adjacent to each other. In essence, the significance of the matrix is to identify shared edges between a pair of triangles in the mesh which is an important parameter in RWG operations.

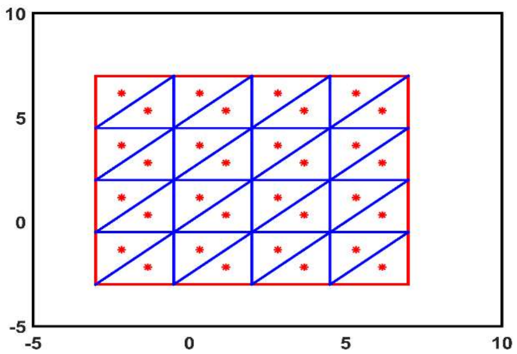

Fig. 10. Sub-dividing a square patch surface into 32 sub-triangles

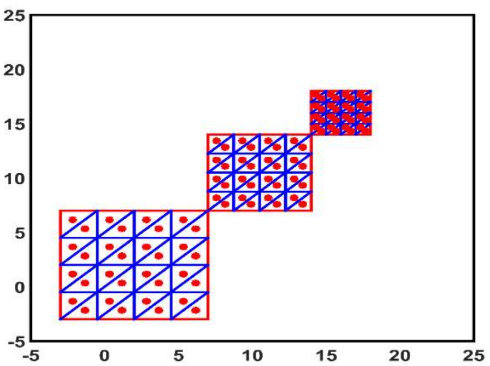

Fig.11. Mesh of different square patch into 32 sub-triangles

$$A = \left[\begin{array}{cccccccccccccccccccccccccccccccc}
0&0&1&0&0&0&0&0&0&0&0&0&0&0&0&0&0&0&0&0&0&0&0&0&0&0&0&0&0&0&0&0 \\
0&0&1&0&0&1&0&0&0&0&0&0&0&0&0&0&0&0&0&0&0&0&0&0&0&0&0&0&0&0&0&0 \\
0&0&0&1&0&0&0&0&0&0&0&0&0&0&0&0&0&0&0&0&0&0&0&0&0&0&0&0&0&0&0&0 \\
0&0&0&0&0&0&0&1&0&0&0&0&0&0&0&0&0&0&0&0&0&0&0&0&0&0&0&0&0&0&0&0 \\
0&0&0&0&0&1&0&0&0&0&1&0&0&0&0&0&0&0&0&0&0&0&0&0&0&0&0&0&0&0&0&0 \\
0&0&0&0&0&0&1&0&0&0&0&0&0&0&0&0&0&0&0&0&0&0&0&0&0&0&0&0&0&0&0&0 \\
0&0&0&0&0&0&0&1&0&0&0&0&1&0&0&0&0&0&0&0&0&0&0&0&0&0&0&0&0&0&0&0 \\
0&0&0&0&0&0&0&0&1&0&0&0&0&0&0&0&0&0&0&0&0&0&0&0&0&0&0&0&0&0&0&0 \\
0&0&0&0&0&0&0&0&0&0&0&0&0&0&1&0&0&0&0&0&0&0&0&0&0&0&0&0&0&0&0&0 \\
0&0&0&0&0&0&0&0&0&0&1&0&0&0&0&0&1&0&0&0&0&0&0&0&0&0&0&0&0&0&0&0 \\
0&0&0&0&0&0&0&0&0&0&0&1&0&0&0&0&0&0&0&0&0&0&0&0&0&0&0&0&0&0&0&0 \\
0&0&0&0&0&0&0&0&0&0&0&0&1&0&0&0&0&0&1&0&0&0&0&0&0&0&0&0&0&0&0&0 \\
0&0&0&0&0&0&0&0&0&0&0&0&0&1&0&0&0&0&0&0&0&0&0&0&0&0&0&0&0&0&0&0 \\
0&0&0&0&0&0&0&0&0&0&0&0&0&0&1&0&0&0&0&0&1&0&0&0&0&0&0&0&0&0&0&0 \\
0&0&0&0&0&0&0&0&0&0&0&0&0&0&0&1&0&0&0&0&0&0&0&0&0&0&0&0&0&0&0&0 \\
0&0&0&0&0&0&0&0&0&0&0&0&0&0&0&0&0&0&0&0&0&0&1&0&0&0&0&0&0&0&0&0 \\
0&0&0&0&0&0&0&0&0&0&0&0&0&0&0&0&0&1&0&0&0&0&0&0&0&0&0&0&0&0&0&0 \\
0&0&0&0&0&0&0&0&0&0&0&0&0&0&0&0&0&0&1&0&0&0&0&1&0&0&0&0&0&0&0&0 \\
0&0&0&0&0&0&0&0&0&0&0&0&0&0&0&0&0&0&0&1&0&0&0&0&0&0&0&0&0&0&0&0 \\
0&0&0&0&0&0&0&0&0&0&0&0&0&0&0&0&0&0&0&0&1&0&0&0&0&1&0&0&0&0&0&0 \\
0&0&0&0&0&0&0&0&0&0&0&0&0&0&0&0&0&0&0&0&0&1&0&0&0&0&0&0&0&0&0&0 \\
0&0&0&0&0&0&0&0&0&0&0&0&0&0&0&0&0&0&0&0&0&0&1&0&0&0&0&1&0&0&0&0 \\
0&0&0&0&0&0&0&0&0&0&0&0&0&0&0&0&0&0&0&0&0&0&0&0&0&0&0&0&0&0&0&0 \\
0&0&0&0&0&0&0&0&0&0&0&0&0&0&0&0&0&0&0&0&0&0&0&0&1&0&0&0&0&0&0&0 \\
0&0&0&0&0&0&0&0&0&0&0&0&0&0&0&0&0&0&0&0&0&0&0&0&0&1&0&0&1&0&0&0 \\
0&0&0&0&0&0&0&0&0&0&0&0&0&0&0&0&0&0&0&0&0&0&0&0&0&0&1&0&0&0&0&0 \\
0&0&0&0&0&0&0&0&0&0&0&0&0&0&0&0&0&0&0&0&0&0&0&0&0&0&0&1&0&0&1&0 \\
0&0&0&0&0&0&0&0&0&0&0&0&0&0&0&0&0&0&0&0&0&0&0&0&0&0&0&0&0&0&0&0 \\
0&0&0&0&0&0&0&0&0&0&0&0&0&0&0&0&0&0&0&0&0&0&0&0&0&0&0&0&0&1&0&0 \\
0&0&0&0&0&0&0&0&0&0&0&0&0&0&0&0&0&0&0&0&0&0&0&0&0&0&0&0&0&0&1&1 \\
0&0&0&0&0&0&0&0&0&0&0&0&0&0&0&0&0&0&0&0&0&0&0&0&0&0&0&0&0&0&0&0 \\
0&0&0&0&0&0&0&0&0&0&0&0&0&0&0&0&0&0&0&0&0&0&0&0&0&0&0&0&0&0&0&0
\end{array}\right] \quad (27)$$

C. Mesh of concentric circular structure using triangular patch

The results of square patch triangulation were presented in the previous sub-section. To approximate a double-ring circular structure at an arbitrary radius, the polar coordinate is translated into the Cartesian coordinate system using the following equations.

$$x_0 = rCos(\theta) \quad (28)$$

$$y_0 = rSin(\theta) \quad (29)$$

$$x_1 = rCos(\theta) + w \quad (30)$$

$$y_1 = rSin(\theta) \quad (31)$$

$$x_3 = rCos(\theta) \quad (32)$$

$$y_3 = rSin(\theta) + h \quad (33)$$

$$x_4 = rCos(\theta) + w \quad (34)$$

$$y_4 = rSin(\theta) + h \quad (35)$$

Eq. (28) – (35) determine the locations of each of the square patches on the circular structure, where the coordinates vary as a function of angle, θ at constant radius, r. Fig.12 shows different plots of double rings circular structure reconstruction. Fig.12(a) shows an assembled or a reconstructed triangular patch of a double-ring circular structure. The inner radius is 4 mm and the outer radius is 9 mm. To approximate the structure using triangular patches, the circular structure was first discretised into 1 x 1 mm small square patches, and each patch was then cut into 32 scalene sub-triangles using barycentric sub-division method.

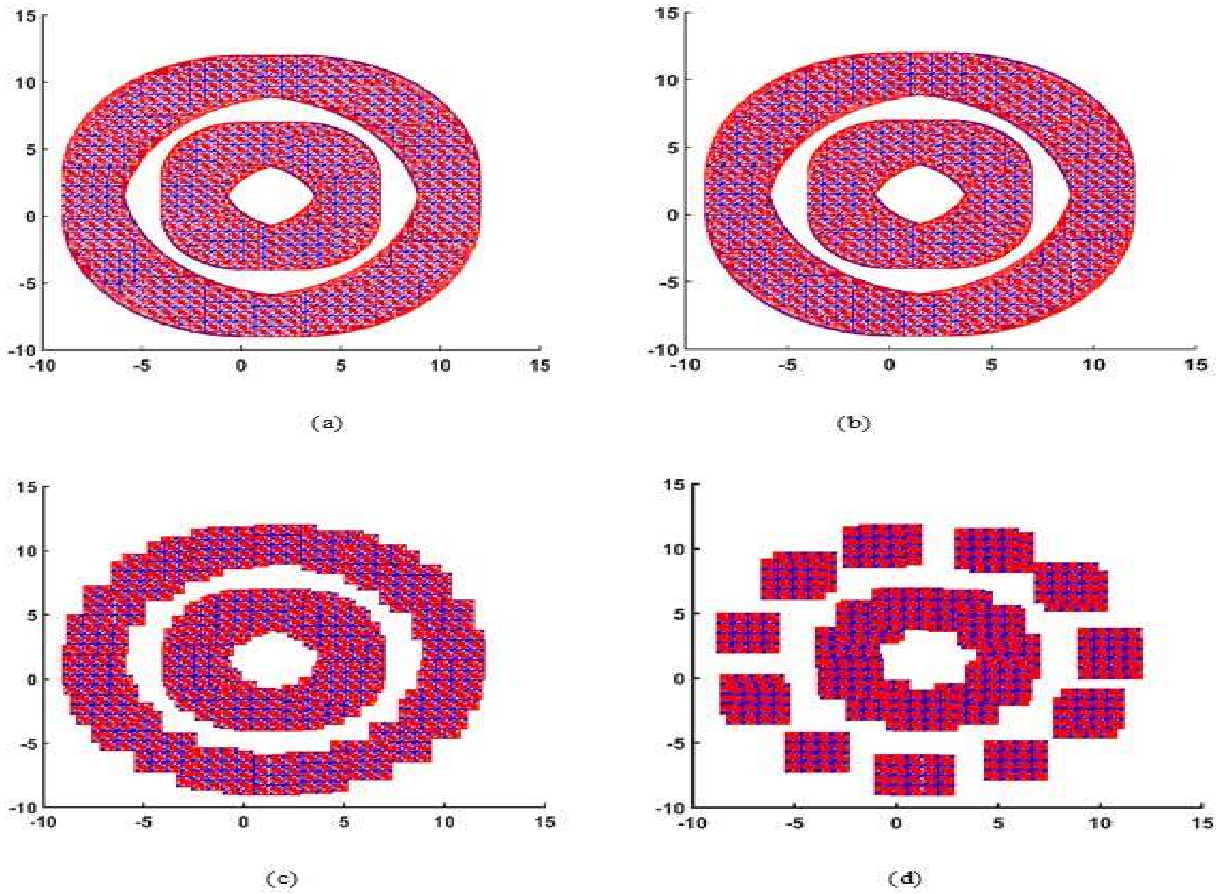

Fig. 11. shows the surface discretization of double rings concentric circle using triangular patch. (a) Double rings of inner radius of 4mm and outer radius of 9mm, square patch of 1mm x 1mm, and angle step of 1 degree, (b) Double rings of inner radius of 4mm and outer radius of 9mm, square patch of 2 x 2mm, and angle step of 1 degree, (c) Double rings of inner radius of 4mm and outer radius of 9mm, square patch of 2x2mm, and angle step of 10 degree, and (d) Double rings of inner radius of 4mm and outer radius of 9mm, square patch of 1mm x 1mm, and angle step of 20 degree.

In Fig.12(b) the dimension used for the square patches was 2 x 2 mm. plots in fig. 12(a) and (b) compute the coordinates at angular step of one (1) degree. Using the same radius, and square patch of 2 x 2 mm, Fig.12(c) shows the reconstructed double rings structure using triangular patches at angular steps of 10 degrees. With a 10-degree step-size, the density of triangular patches is less than that of 1-degree step. Similarly, fig.12(d) shows the reconstructed double circular rings using triangular patches at 20-degree step increments.

IV. CONCLUSION

In this paper, division of a primary triangles into sixteen (16) sub-triangles to provide approximate mesh structure for a square patch and circular shaped double rings structure is presented. By iterative sub-division of adjacent edges along their mean values, and connecting them to insert a new edge, an isosceles triangle can be sub-divided into scalene sub-triangle. Imposing a constraint on the edge length to search for shared edges, a connectivity matrix is constructed. The method demonstrates that square and circular structures can be reconstructed using mesh. The quality of the reconstructed mesh structure depends on the density of the triangular patches and the step angle used.

REFERENCES

Andriulli, F. P.; F. Vipiana and G. Vecchi. (2008). Hierarchical bases for nonhierarchic 3-D triangular meshes. *IEEE Transactions on Antennas and Propagation*, *56*(8), 2288-2297.

Anisimov, D.; C. Deng and K. Hormann. (2016). Subdividing barycentric coordinates. *Computer Aided Geometric Design*, *43*, 172-185.

Bauer, M.; N. Charon; P. Harms and H.W. Hsieh. (2021). A numerical framework for elastic surface matching, comparison, and interpolation. International Journal of Computer Vision, 129(8): 2425-2444.

Bertrand, M.; G. Valerio; M. Ettorre and M. Casaletti (2019). RWG basis functions for accurate modeling of substrate integrated waveguide slot-based antennas. IEEE Transactions on Magnetics, 56(1). 1-4.

Blu, T.; P. Thévenaz and M. Unser. (2004). Linear interpolation revitalized. *IEEE Transactions on Image Processing*, *13*(5). 710-719.

Diaconis, P., and Miclo, L. (2011). On barycentric subdivision. *Combinatorics, Probability and Computing*, *20*(2): 213-237.

Ding, N.; L. Yin; X. Zhao; Z. Lin; Y. Zhang; A. Luo and X. Dang. (2024). An efficient adaptive h-refinement for the RWG-based electric field integral equation applied to antennas with waveport. IET Microwaves, Antennas & Propagation, 18(3). 155-163.

Gassner, G. J. and Winters, A. R. (2021). A novel robust strategy for discontinuous Galerkin methods in computational fluid mechanics: Why? When? What? Where? Frontiers in Physics, 8, 500690.

Gibson, W. C. (2021). The method of moments in electromagnetics. Chapman and Hall/CRC.

Gurel, L., and Ergul, O. (2009). Contamination of the accuracy of the combined-field integral equation with the discretization error of the magnetic-field integral equation. *IEEE transactions on antennas and propagation*, *57*(9): 2650-2657.

Harrington, R. F. (1987). The method of moments in electromagnetics. Journal of Electromagnetic waves and Applications, 1(3): 181-200.

Hennig, P., and Schuler, C. J. (2012). Entropy search for information-efficient global optimization. *Journal of Machine Learning Research*, *13*(6).

Hernández-Lobato, J.; M.W. Hoffman and Z. Ghahramani. (2014). Predictive entropy search for efficient global optimization of black-box functions. *Advances in neural information processing systems*, *27*.

Hormann, K., and Greiner, G. (2000). MIPS: An efficient global parametrization method. *Curve and Surface Design: Saint-Malo 1999*: 153-162.

Huang, S. W.; G.H. Zhang; M.Y. Xia and C.H. Chan (2009). Numerical analysis of scattering by dielectric random rough surfaces using modified SMCG scheme and curvilinear RWG basis functions. IEEE transactions on antennas and propagation, 57(10). 3392-3397.

Ju, T.; S. Schaefer and J. Warren (2023). Mean value coordinates for closed triangular meshes. In Seminal Graphics Papers: Pushing the Boundaries, 2: 223-228

Ju, T.; S. Schaefer and J. Warren (2023). Mean value coordinates for closed triangular meshes. In *Seminal Graphics Papers: Pushing the Boundaries, Volume 2* (pp. 223-228).

Koam, A. N., and Ahmad, A. (2020). Barycentric subdivision of Cayley graphs with constant edge metric dimension. *IEEE Access*, *8*: 80624-80628.

Li, J. Y. and Li, L. W. (2004). Electromagnetic scattering by a mixture of conducting and dielectric objects: Analysis using method of moments. IEEE transactions on vehicular technology, 53(2). 514-520.

Li, J.; L. Zhang and Q.H. Qin. (2021). A regularized method of moments for three-dimensional time-harmonic electromagnetic scattering. Applied Mathematics Letters, 112, 106746.

Liu, R.; G. Xiao and Y.Hu. (2024). Solving Surface-volume Integral Equations for PEC and Inhomogeneous/Anisotropic Materials with Multibranch Basis Functions. The Applied Computational Electromagnetics Society Journal (ACES). 108-114.

Liu, Z.; Y. Feng; M.J. Black; D. Nowrouzezahrai; L. Paull and W. Liu. (2023). Mesh diffusion: Score-based generative 3d mesh modeling. *arXiv preprint arXiv:2303.08133*.

Luo, Q. and Wang, J. (2020). On the density of shapes in three-dimensional affine subdivision. AIMS Mathematics, 5(5), 5381-5388.

Lu, M. and Michielssen, E. (2002, June). Closed form evaluation of time domain fields due to Rao-Wilton-Glisson sources for use in marching-on-in-time based EFIE solvers. In IEEE Antennas and Propagation Society International Symposium (IEEE Cat. No. 02CH37313), 1. 74-77. IEEE.

Luo, W.; J. Liu; Z. Li and J. Song. (2020). Efficient triangular interpolation methods: Error analysis and applications. IEEE Antennas and Wireless Propagation Letters, 19(6). 1032-1036.

Munkberg, J.; J. Hasselgren; T. Shen; J. Gao; W. Chen;A. Evans ... and S. Fidler. (2022). Extracting triangular 3d models, materials, and lighting from images. In *Proceedings of the IEEE/CVF Conference on Computer Vision and Pattern Recognition*. 8280-8290.

Niino, K. and Yamamoto, S. (2024). The Galerkin method for a regularised combined field integral equation without a dual basis function. arXiv preprint arXiv:2406.07924.

Øyre, E. S. (2021). Electromagnetic Scattering Calculations for Arbitrarily Shaped Closed Surfaces using the Method of Moments (Master's thesis, NTNU).

Oostendorp, T. F.; A. van Oosterom and G, Huiskamp. (1989). Interpolation on a triangulated 3D surface. Journal of Computational Physics, 80(2). 331-343.

P elamatti, J.; L. Brevault; M. Balesdent; E.G. Talbi and Y. Guerin. (2019). Efficient global optimization of constrained mixed variable problems. *Journal of Global Optimization*, *73*:583-613.

Peng, S.; C. Jiang; Y. Liao; M. Niemeyer; M. Pollefeys and A. Geiger. (2021). Shape as points: A differentiable poisson solver. *Advances in Neural Information Processing Systems*, *34*: 13032-13044.

Rao, S. M. (2024). A Simple, Method of Moments Solution for the Integral Equations for Multiple Dielectric Bodies of Arbitrary Shape in Time Domain. Applied Computational Electromagnetics Society Journal (ACES). 201-214.

Rao, S.; D. Wilton and A. Glisson. (1982). Electromagnetic scattering by surfaces of arbitrary shape. IEEE Transactions on antennas and propagation, 30(3). 409-418.

Rao, S.; D. Wilton and A. Glisson. (1982). Electromagnetic scattering by surfaces of arbitrary shape. IEEE Transactions on antennas and propagation, 30(3), 409-418.

Romanowska, A. B.; J.D.H. Smith and A. Zamojska-Dzienio. Barycentric algebras and barycentric coordinates. J. Carr–Algebraically Describing Color Trades on Complete Bipartite Graphs 7, 22.

Rius, J. M.; E. Ubeda and J. Parrón (2001). On the testing of the magnetic field integral equation with RWG basis functions in method of moments. IEEE Transactions on Antennas and Propagation, 49(11). 1550-1553.

Thiery, J. M.; J. Tierny and T. Boubekeur. (2014). Jacobians and Hessians of mean value coordinates for closed triangular meshes. The Visual Computer, 30. 981-995.

Ubeda, E.; I. Sekulic; J.M. Rius and A. Heldring. (2020). Accurate, grid-robust and versatile combined-field discretization for the electromagnetic scattering analysis of perfectly conducting targets. Journal of Computational Physics, 407. 109236.

Ubeda, E.; J.M. Rius and A. Heldring. (2014). Nonconforming discretization of the electric-field integral equation for closed perfectly conducting objects. *IEEE Transactions on Antennas and Propagation*, *62*(8):4171-4186.

Ubeda, E.; J.M. Rius; A. Heldring and I. Sekulic. (2015). Volumetric testing parallel to the boundary surface for a nonconforming discretization of the electric-field integral equation. *IEEE Transactions on Antennas and Propagation*, *63*(7): 3286-3291.

Wongwaen, N.; S. Tiendee and C. Sinthanayothin. (2012, June). Method of 3D mesh reconstruction from point cloud using elementary vector and geometry analysis. In 2012 8th International Conference on Information Science and Digital Content Technology (ICIDT2012) (Vol. 1, pp. 156-159). IEEE.

Wilton, D. R.; S.M. Rao and A.W. Glisson. (1982). Electromagnetic scattering by surfaces of arbitrary shape. IEEE Transactions on Antennas and propagation, 30(3). 409-418.

Xiang, C.; X. Dang; M. Li; F. Yang and S. Xu. (2020). Application of barycentric subdivision method for singularity integration in method of moments. The Applied Computational Electromagnetics Society Journal (ACES). 250-257.